SAND2022-16771C

Top-Down Control Design Strategy for Electric Power Grid EMP (E3) Protection

Timothy J. Donnelly
Sandia National Laboratories
Albuquerque, NM
tjdonne@sandia.gov

David G. Wilson
Sandia National Laboratories
Albuquerque, NM
dwilso@sandia.gov

Rush D. Robinett III
Michigan Technological University
Houghton, MI
rdrobine@mtu.edu

***Abstract*—A high altitude electromagnetic pulse (HEMP) caused by a nuclear explosion has the potential to severely impact the operation of large-scale electric power grids. This paper presents a top-down mitigation design strategy that considers grid-wide dynamic behavior during a simulated HEMP event – and uses optimal control theory to determine the compensation signals required to protect critical grid assets. The approach is applied to both a standalone transformer system and a demonstrative 3-bus grid model. The performance of the top-down approach relative to conventional protection solutions is evaluated, and several optimal control objective functions are explored. Finally, directions for future research are proposed.**

Keywords—High Altitude Electromagnetic Pulse (HEMP), Geomagnetically Induced Currents (GIC), saturating transformer, optimal control

I. Introduction

Today a variety of both natural and man-made high impact, low frequency (HILF) events threaten the reliable operation of the electric power grid – these events include such things as extreme weather, cyber-attacks, and coordinated physical disturbances [1]. In addition, there is growing concern regarding the threats to the electric power grid posed by high-altitude electromagnetic pulses (HEMPs) and solar-geomagnetic disturbances (GMDs) [1]-[5]. During these geomagnetic events, changes in the earth's magnetic field (caused by a high-altitude nuclear explosion or charged particles from a coronal mass ejection) result in a slowly varying electric field at the earth's surface. Power grid equipment, which is dispersed across large geographic areas and interconnected with long transmission lines, becomes susceptible to these slowly varying fields.

One major component of the electrical insults caused by HEMP/GMD events are geomagnetically-induced currents (GICs) flowing through large power transformers. These GICs are much lower in frequency than the 50/60 Hz ac currents that such equipment is designed to handle. Thus, these currents can introduce a magnetic flux offset in the core of the transformer which can result in the transformer becoming severely saturated. This saturation significantly deteriorates the performance of the transformer, leading to distorted ac waveforms, increased losses, and the potential for thermal damage [4]-[6]. It is also possible that system-level cascading failures may occur as a result of compounding effects [7].

Over the years, several strategies for mitigating the impacts of a geomagnetic event have been evaluated. A common approach that has been proposed is inserting a blocking capacitor between transformer neutral and ground [8]-[10]. This blocking capacitor can be sized to be a relatively large impedance in the GMD frequency range (mHz) – thus blocking GICs, but remain a low impedance in the 50/60Hz range – which is useful for system voltage balance and fault detection considerations. In addition to blocking capacitors, two recent approaches to mitigating the impact of a HEMP/GMD event have also been investigated: the use of externally excited tertiary windings to neutralize geomagnetically-induced magnetic core flux offsets [11], and the use switching devices instead of a passive blocking capacitors in the neutral path [12][13].

This paper builds on these research findings and proposes a new *top-down* approach for designing and evaluating HEMP/GMD mitigation strategies. Instead of focusing on specific mitigation technologies (e.g., blocking capacitors), the top-down approach generalizes the problem and formulates the task of mitigating the impact of a HEMP event as an optimal control design challenge. This enables the established tools and techniques from optimal control theory to be applied, and also serves as a foundation for a rigorous and systematic design approach. It is envisioned that this top-down approach could provide new insights/strategies to help mitigate the HEMP threat, and that the resulting optimal control solutions can drive practical design specifications for future grid applications.

The remainder of this paper is organized as follows: Section II provides an overview of the transformer model and outlines the optimal control problem formulation. Section III provides simulation results for a standalone transformer system that is subjected to a simulated EMP/E3a pulse, and the behavior of several control strategies are evaluated. Section IV extends the standalone transformer case-study and considers a small-scale 3-bus power system. The potential consequences of using controls to protect one transformer but not a neighboring transformer are evaluated, and a new objective function is proposed to minimize these consequences. Finally, conclusions and directions of future research are provided in Section V.

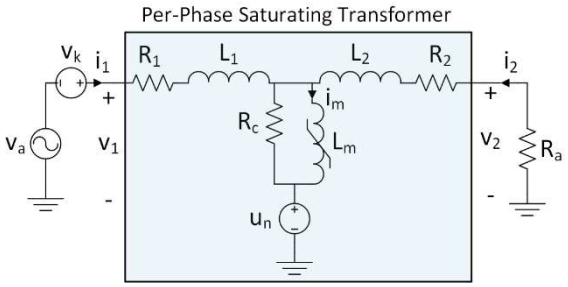

Fig. 1 – Saturating transformer model

This work was supported by the Department of Energy's Office of Cybersecurity, Energy Security, and Emergency Response (CESER) with funding under the Laboratory Award: *EMP/GMD Modeling and Assessments; Testing and Validation; and Mitigation*

II. Transformer Model and Optimal Control Formulation

A. Saturating Transformer Model

The nonlinear saturating transformer model is highlighted in Fig. 1. Therein, the components R_1, R_2, L_1, L_2 correspond to the traditional primary- and secondary-side winding resistances and leakage inductances, respectively. The core of the device is modeled by a nonlinear magnetizing inductance L_m, and core losses are accounted for by the resistor R_c. Finally, the voltage source u_n represents an added component that sits between the transformer neutral and ground. This voltage source can represent a grounded neutral ($u_n = 0$), a neutral blocking capacitor ($\dot{u}_n = (i_1 + i_2)/C_b$), or more generally any desired control signal. Overall, the transformer model is defined by the dynamic equations given in (1)

$$\begin{aligned} L_1\dot{i_1}(t) &= -(R_1 + R_c)i_1 - R_c(i_2 + i_m) + v_1 - u_n \\ L_2\dot{i_2}(t) &= -(R_2 + R_c)i_2 - R_c(i_1 + i_m) + v_2 - u_n \\ \dot{\lambda_m}(t) &= R_c(i_1 + i_2 - i_m) \end{aligned} \quad (1)$$

which can be written as $\dot{x}(t) = f(x(t), u(t))$, where $x = [i_1, i_2, \lambda_m]$ and $u = u_n$. To use (1), an additional algebraic equation that defines the relationship between the magnetizing current i_m and the magnetizing flux linkage, λ_m is also needed. Here, a tangent function was used as a simple approximation to an anhysteretic B-H curve:

$$i_m = k_1 \tan(k_2 \lambda_m) \quad (2)$$

where k_1 and k_2 are user selected constants. A plot of (2) is shown in Fig. 2 and it is noted that k_1 and k_2 were selected to match the piecewise-linear inductance provided in [14] at the two points where the slope is indicated. The other parameters for the transformer model are listed in TABLE I.

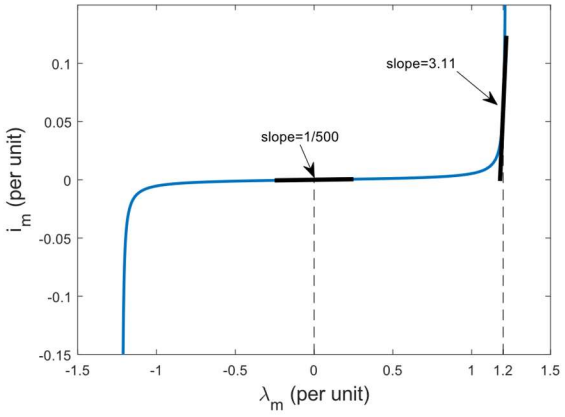

Fig. 2 – B-H curve based on tanget function

TABLE I. Transformer Parameters

Parameter	Value
R_1, R_2	0.2% (per unit, p.u.)
L_1, L_2	8% (p.u.)
R_c, R_a	500, 1 (p.u.)
k1, k2	0.0016, 1.2879

B. Optimal Control Formulation

Optimal control theory is broadly concerned with finding a control signal, $u(t)$, such that the dynamic behavior of the combined control and plant system minimizes a given objective function, J. A common choice for J is a functional that integrates its argument, $F(\cdot)$, over time. The optimal control problem formulation used in this work is given in (3).

$$\min_{x(t),u(t)} J = \int_{t_0}^{t_f} F(x(t), u(t), t)dt$$

such that, (3)

$$\dot{x}(t) = f(x(t), u(t))$$

$$lb \le g\big(x(t), u(t)\big) \le ub$$

In (3), the minimization problem is augmented by additional constraints: the system state must satisfy the system dynamic equations, $\dot{x} = f(\cdot)$, and a provision is also provided for a user defined path constraint, $g(\cdot)$, that is limited to the range $[lb\ ub]$.

III. StandAlone Transformr Case Study

As a preliminary case-study for applying optimal control theory to the study of EMP grid resilience, the standalone transformer system shown Fig. 1 is considered. The transformer in this system is supplied on the primary side by two voltage sources, v_a and v_k. They represent a 60Hz ac signal and a simulated EMP pulse, respectively. The secondary side of the transformer is terminated with a fixed resistance, R_a.

An EMP pulse is typically described as having three distinct phases: E1, E2, and E3 which are differentiated based on the magnitude and frequency content of that phase of the pulse. The late-time E3 component is the longest lasting (on the order of seconds to minutes), and thus is the most impactful in terms of generating GICs [15]. Moreover, the E3 phase can be subdivided into the blast (E3a) and heave components (E3b). Although both impact transformer/GIC behavior, only the E3a component is considered here for demonstration purposes – however the same techniques could be applied for the E3b component as well. The characteristics of the E3a waveform are provided in [15] and a reproduced illustration of the waveform is shown in Fig. 3.

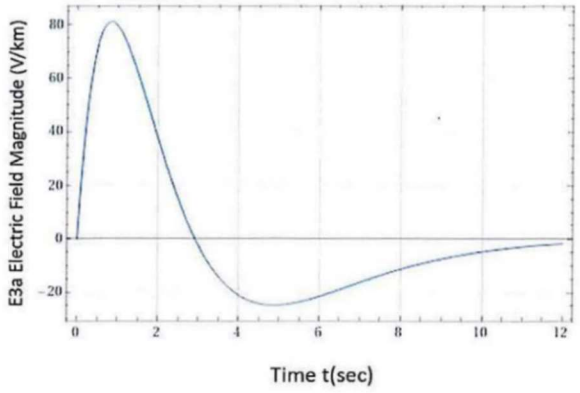

Fig. 3 – Dept. of Energy E3a waveform [15]

A. Conventional Mitigation Strageties

To study the behavior of the standalone transformer in response to the E3a impulse, the differential equations of the transformer were implemented in MATLAB and the ODE solver `ode15s` was then used to simulate to system over a 20 second time interval. Initially, the system was simulated with no control mitigation ($u_n = 0$) and no ac component ($v_a = 0$) [AC simulations are deferred to the Appendix]. The behavior of the magnetizing flux in the core of the transformer during this interval is shown in Fig. 4 (labeled: no mitigation). In this case, the E3a pulse pushes the transformer well into saturation. For reference, the 1.2 p.u. saturation level is indicated in Fig. 4 with horizontal dashed lines.

To compare the $u_n = 0$ study, a neutral blocking capacitor study was also conducted. The neutral blocking capacitor was added to the simulation by including the ODE and initial condition:

$$\dot{u}_n = (i_1 + i_2)/C_b,\ u_n(0) = 0$$

where C_b was selected to be 1Ω at 60Hz (2.65mF) [16]. The results of this study are shown in Fig. 4 (labeled: blocking capacitor). The blocking capacitor generally does a suitable job at preventing the transformer from becoming severely saturated, although saturation does occur up to the 1.2 p.u. level indicated. The control signal u_n (in this case, the blocking capacitor voltage) is shown in Fig. 5. It is noted from a control's perspective, the blocking capacitor can be thought of as an integrator feedback on the neutral current.

B. Optimal Mitigation Strategies

Two additional studies of the standalone transformer system were conducted. These studies used optimal control techniques to shape the behavior of the transformer in response to the E3a impulse. The first optimal controller considered was a linear quadratic regulator (LQR). The LQR uses feedback in the form

$$u_n = -Kx$$

and provides an optimal solution to (3), assuming the system dynamics are linear, the cost function is a quadradic, and no path constraints are present.

For this demonstration, the transformer dynamics given in (1) were linearized and a cost function $F = \lambda_m^2 + \beta u_n^2$ was assumed. The MATLAB function `lqr` was used to determine the gain K, and the state-feedback controller was incorporated into the nonlinear dynamic simulation. The resulting magnetizing flux and control signal are shown in Figs. 4 and 5, respectively (labeled: LQR). The cost function parameter β was adjusted so that the peak magnetizing flux matched the case for the blocking capacitor. Overall, the LQR smoothly recovers to the E3a impulse.

Finally, the more general optimal control problem (3) – which can directly account for nonlinear dynamics and include path constraints – was solved for the standalone transformer system. The problem was formulated to limit transformer magnetizing flux to between ±1.2 p.u., while doing so with minimal control effort: i.e., $-1.2 \le g = \lambda_m \le 1.2$, $F = u_n^2$. The optimal control problem was solved using direct collocation techniques, which discretizes the system dynamics and objective function and turns (3) into a standard mathematical optimization problem [17]. The third-party MATLAB package `optimTraj` [18] was used to perform the direct collocation, which was modified internally to use the IPOPT nonlinear solver [19][20].

The resulting magnetizing flux λ_m and control signal u_n for the optimal solution are shown in Figs. 4 and 5, respectively (labeled: λ_m limit). It is noted that the solution specifies u_n at time $t = 0$ to be a positive/non-zero value. This drives the magnetizing flux negative initially, and thus preemptively counter acts the E3a impulse. Throughout the rest of the interval, the magnetizing flux is minimally controlled and thus runs into both the positive and negative saturation limits as the E3a pulse passes.

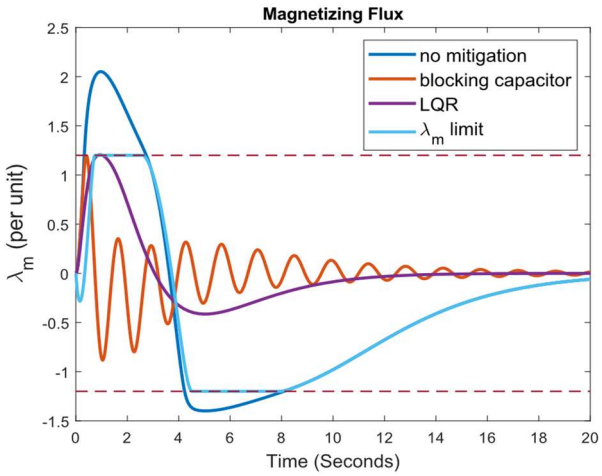

Fig. 4 – Transformer flux in response to an E3a impulse

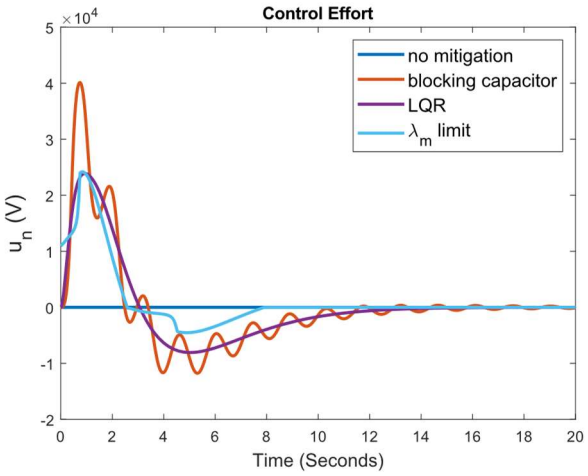

Fig. 5 – Control voltage injected in transformer neutral

IV. Small Power System Case Study

The standalone transformer system considered in Section III provides a useful demonstration of the top-down HEMP/E3 mitigation strategy proposed in this work. However, further insights can be obtained by considering a slightly more involved grid configuration.

A single-line diagram of the 3-bus power system is shown in Fig. 6. The system consists of a generator/step-up transformer, a long (350km) transmission line, and two parallel load transformers. The two load transformers are labeled Transformer A and B, respectively and are separated by a short 50km transmission line. The same saturating transformer model considered in Section III is used here for all three transformers.

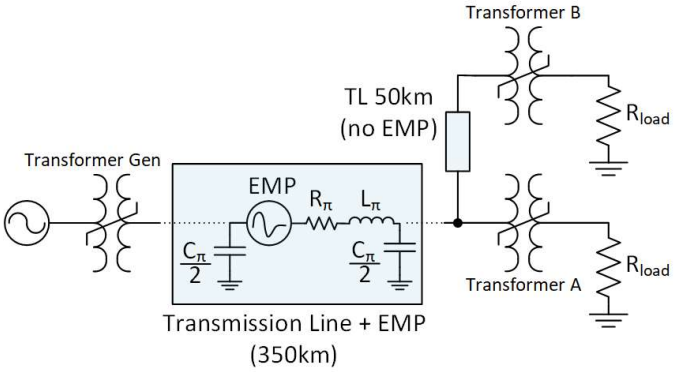

Fig. 6 – A 3-bus power grid model with simulated EMP insult

The simulated effects of a HEMP event are incorporated into the grid by embedding a E3a voltage source (Fig. 3) in the transmission line model. For simplicity, it is assumed that the EMP has an east-west orientation and only couples to the long line. Pi-equivalent circuits are used to model the transmission lines, and the parameters are listed in TABLE II [21].

TABLE II. TRANSMISSION LINE PARAMETERS

Parameter	Value
R_π	0.01273Ω/km
L_π	0.9337mH/km
C_π	12.47nF/km

A. Dual Transformer Protection

The analysis of the 3-bus power system begins with a simulation and optimal control study in which both load transformers (A & B) are treated equally in terms of EMP mitigation.* Fig. 7 and Fig. 8 show the results of this study, showing the magnetizing flux and control signals, respectively. Within these, four case studies were considered: no mitigation, blocking capacitors, LQR, and optimal controllers based on path constraints (λ_m limits).

Overall, it is noted that the 3-bus system behaves similarly to the standalone transformer case study. Like in Section III, with no mitigation in place the E3a pulse pushes the unprotected transformers well into saturation. Likewise, with the blocking capacitors in place, the magnetizing flux is limited to approximately 1.2 p.u. The primary difference between the two blocking capacitor studies is that the response is slightly more damped in the 3-bus system compared to the single transformer system, likely due to circuit topology and the added resistance introduced by the transmission lines.

The primary difference between the 3-bus system and standalone system as far as the optimal control formulation is concerned is that the control signal now has two components: a separate u_n for each load transformer (i.e., $u = [u_{n,A}, u_{n,B}]$). The path constraints and objective function were modified to account for the added control signal dimension, but overall the same strategy was utilized. Both optimal controllers behave in a similar way to the standalone transformer study in Section III.

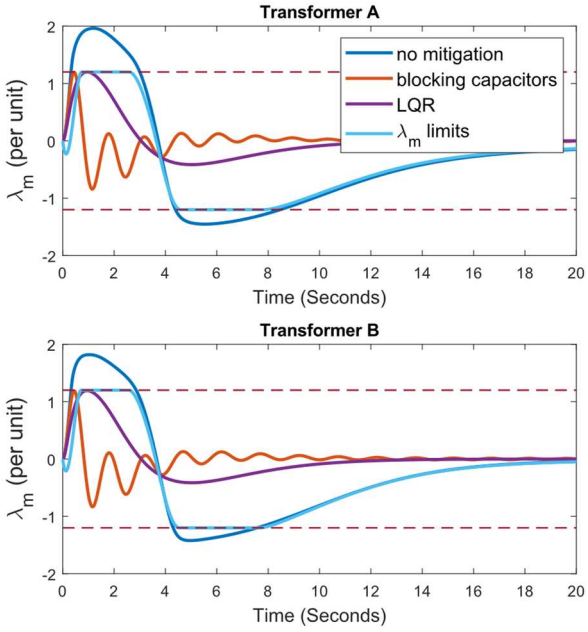

Fig. 7 – Load transformer flux for 3-bus power system

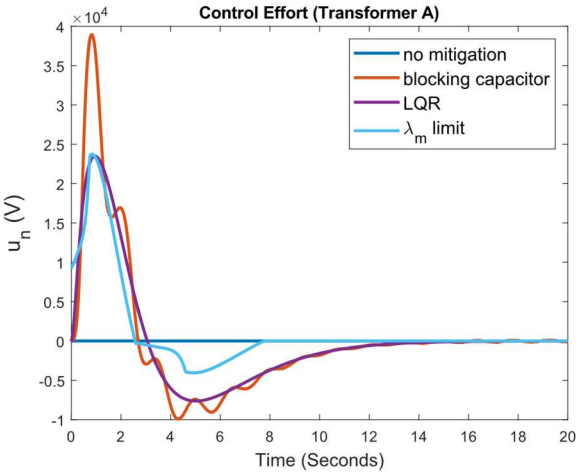

Fig. 8 – Control voltage injected in load transformer neutral (only $u_{n,A}$ shown for brevity, $u_{n,B}$ had similar behavior)

B. Single Transformer Protection

A concern that has been raised in the literature regarding transformer EMP/GMD protection is the issue that protecting only a subset of transformers in a system might cause the incident wave at unprotected transformers to be exacerbated [7]. This phenomenon has been termed "GIC shifting," and is

* The step-up transformer is assumed throughout to have no EMP mitigation ($u_{n,gen} = 0$), since it is the only return path for GICs and thus its role is similar in nature to the standalone transformer case-study considered in Section III

fundamentally due to current finding the path of least impedance [9]. This scenario is studied for the 3-bus system shown in (3) by enforcing $u_{n,B} = 0$ and only considering the impact that $u_{n,A}$ has. The same four mitigation strategies considered in Section IV-A are considered here; Fig. 9 and Fig. 10 show the results for: no mitigation, blocking capacitor, LQR, and an optimal controller based on strict λ_m limits. A fourth optimal controller (labeled: min-max saturation) was also considered and will be discussed.

The results for the no mitigation study are unchanged from Section IV-A. However, with the blocking capacitor the GIC shifting issue is put clearly on display: the single capacitor does an acceptable job of limiting saturation in Transformer A, but at the cost of saturating Transformer B even more than the base-case study (up to approximately 2.4 p.u., vs. 1.8 p.u. for the no mitigation study).

Likewise, the LQR controller and optimal controller based on λ_m limits also suffer from GIC shifting. For the LQR controller, an objective function $F = \lambda_{m,A}^2 + \lambda_{m,B}^2 + \beta u_n^2$ was used where $\lambda_{m,A}$, $\lambda_{m,B}$ correspond to the magnetizing flux in Transformers A & B, respectively. Linear analysis of the system dynamics reveals that the system is not controllable with only one control input ($u = u_{n,A}$), thus even with a negligible penalty on expended control effort ($\beta = 10^{-9}$), Transformer B is still pushed into a severe saturation regime. The optimal controller based on limits λ_m limits behaves similarly: the magnitude of Transformer A's magnetizing flux is kept to at or below 1.2 p.u., but Transformer B's flux is pushed deeper into saturation than the no mitigation study (~2.1 p.u. vs. 1.8 p.u., respectively).

To alleviate the GIC shifting phenomenon, a third optimal controller is proposed with an alternative objective function. The new objective function is based around the idea of limiting the total transformer saturation over the E3a interval. For a single transformer, a measure of the total saturation can be defined as in (4), which gives the area between the λ_m curve and a constant λ_{sat}, for intervals in which the magnitude of λ_m is greater than λ_{sat}.

$$\text{saturation area} \equiv \int \max\left(|\lambda_m| - \lambda_{sat}, 0\right) dt \tag{4}$$

Equation (4) applies to a single transformer, but can also be extended to multiple transformers by adding additional terms to the max() function. E.g., for 3-bus system the saturation area is given by:

$$\text{s. a.} \equiv \int \max\left(\left|\lambda_{m,A}\right| - \lambda_{sat,A}, \left|\lambda_{m,B}\right| - \lambda_{sat,B}, 0\right) dt \tag{5}$$

In (5), the integrand will return the greater between $\left|\lambda_{m,A}\right| - \lambda_{sat,A}$ and $\left|\lambda_{m,B}\right| - \lambda_{sat,B}$ (and 0), and thus provides a measure of the transformer saturation at a system-level.

This system-level transformer saturation objective is demonstrated for the 3-bus system by using the formula given in (5) as the objective function in (3). Since the objective function must be a smooth continuous function, the max() function is reformulated by introducing a dummy variable, u_t, and minimizing u_t under the constraint that it must be greater than each of the original arguments of the max() function. The full form of the optimal control problem is given by:

$$\min_{x(t),u(t)} \int_{t_0}^{t_f} (u_t + \gamma u_{n,A}^2) dt$$

such that, (6)

$$\dot{x}(t) = f(x(t), u(t), t)$$

$$u_t \geq 0,\ u_t \geq \left|\lambda_{m,A}\right| - \lambda_{sat,A},\ u_t \geq \left|\lambda_{m,B}\right| - \lambda_{sat,B}$$

where $u = [u_{n,A},\ u_t]$ and the term $\gamma u_{n,A}^2$ was added to the objective function for regularization purposes ($\gamma = 10^{-7}$).

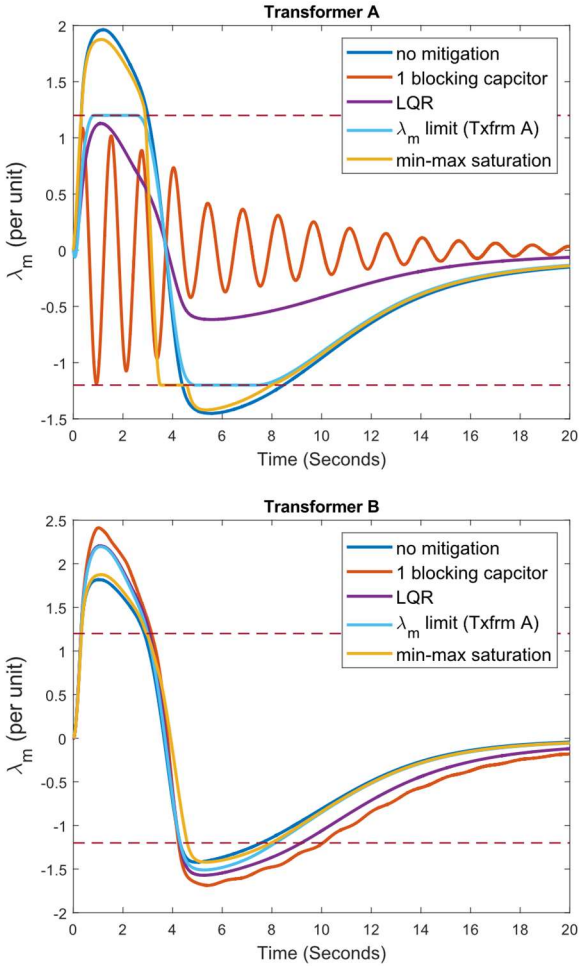

Fig. 9 – Transformer flux for the 3-bus grid (only Transformer A has EMP protection)

The load transformer magnetizing fluxes and $u_{n,A}$ optimal solution to (6) are shown in Fig. 9 and Fig. 10, respectively (labeled: min-max saturation). For this solution, saturation in Transformers A and B were treated with equal concern: $\lambda_{sat,A} = \lambda_{sat,B} = 1.2$ per unit. The primary difference between this solution and the other mitigation solutions (blocking-capacitor & λ_m limit) is that the GIC shifting phenomenon is no longer present.

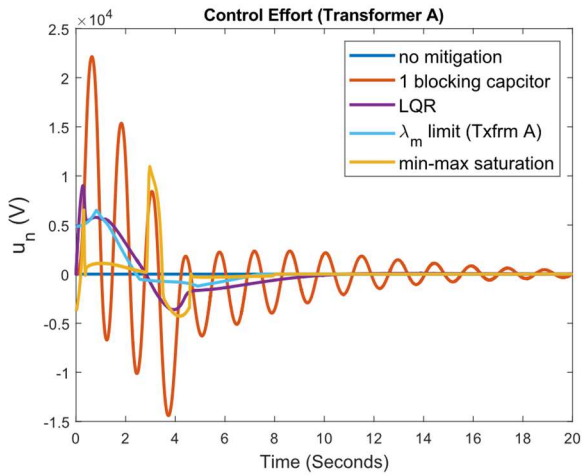

Fig. 10 – Transformer A neutral control voltage

Instead, for the first part of the interval, the min-max solution generally follows the same trajectory as the no-mitigation study. However, a small control is being applied during this time ($t < 3$) which reduces the peak magnetizing flux in Transformer A compared to the no mitigation case. At $t = 3$, the transformer control signal jumps to a large positive value which quickly reduces the magnetizing flux in Transformer A until it reaches -1.2 per unit. Immediately after, the sign of the control signal is reversed and a -1.2 per flux in Transformer A is maintained. Because the flux in Transformer A was driven quickly to -$\lambda_{sat,A}$ (faster than the natural response to the E3a impulse), the flux in Transformer B is allowed to more gradually decrease. Ultimately, this leads Transformer B spending less time below -1.2 p.u. than the no mitigation base case study. A comparison of the saturation area calculated via Eq. (5) for the various controllers is shown in TABLE III.

TABLE III. 3-BUS TRANSFORMER SATURATION (WITH $u_{n,B} = 0$)

Study	Saturation Area
no mitigation	2.134 (p.u.)
1 blocking capacitor	3.994 (p.u.)
LQR	3.048 (p.u.)
λ_m limit (Txfrm A)	2.588 (p.u.)
min-max saturation	1.719 (p.u.)

C. Discussion

The EMP mitigation studies for the 3-bus power system demonstrate two important findings: (1) it is possible to limit saturation in both load transformers if they each incorporate some form of protection (blocking capacitor or optimal controller), and (2) if only one transformer is protected a trade-off must be made between protecting only the local transformer and attempting to protect both transformers.

From a practical perspective, it is clear from Fig. 7 and Fig. 9 that if one is going to add EMP mitigation to the 3-bus system, there is a clear advantage to adding protection to both load transformers instead of only one. This conclusion is enabled by the top-down approach, which showed that even an optimal controller that was purposefully designed to minimize saturation in both transformer is only able to achieve moderately less saturation than when no protection was applied at all.

More broadly, however, the top-down approach enables a unified way to understand the tradeoffs when investigating various EMP protection solutions. It is quite possible, for example, that for larger and/or different power system topologies, an acceptable compromise between the number of transformers protected and that saturation that each transformer experiences could be obtained. This topic, along with identifying potentially better objective and constraint functions, serves a proposed area of future research.

V. CONCLUSION

A top-down design approach for developing transformer EMP/GMD protection based on optimal control theory is described in this paper. The approach is demonstrated on both a standalone transformer system and 3-bus grid model. Overall, the approach is shown to provide a unified way to evaluate the dynamic behavior of given system, and initial steps towards developing controls which outperform conventional solutions are outlined. Future research aims to further develop the technique by considering larger power grid models and investigating advanced feedback control architectures.

VI. ACKNOWLEDGMENT

Sandia National Laboratories is a multimission laboratory managed and operated by National Technology & Engineering Solutions of Sandia, LLC, a wholly owned subsidiary of Honeywell International Inc., for the U.S. Department of Energy's National Nuclear Security Administration under contract DE-NA0003525. This paper describes objective technical results and analysis. Any subjective views or opinions that might be expressed in the paper do not necessarily represent the views of the U.S. Department of Energy or the United States Government. The authors would like to thank Julia Tilles and Jon Rogers for their leadership and technical input related to the content and direction of this work.

REFERENCES

[1] Weiss, M., Weiss, M. An assessment of threats to the American power grid. Energ Sustain Soc 9, 18 (2019). https://doi.org/10.1186/s13705-019-0199-y

[2] H. M. Pennington, C. J. Hanley and J. D. Rogers, "Toward an Electromagnetic Event Resilient Grid," in *Proceedings of the IEEE*, vol. 109, no. 4, pp. 315-319, April 2021, doi: 10.1109/JPROC.2021.3062297

[3] "Perspectives on Protecting the Electric Grid from an Electromagnetic Pulse or Geomagnetic Disturbance," Hearing of the U.S. Senate Homeland Security and Governmental Affairs Committee 2019 (Dr. Randy Horton)

[4] Magnetohydrodynamic Electromagnetic Pulse Assessment of the Continental U.S. Electric Grid: Geomagnetically Induced Current and Transformer Thermal Analysis. EPRI, Palo Alto, CA: 2017. 3002009001.

[5] J. G. Kappenman, "Geomagnetic Storms and Their Impact on Power Systems," in IEEE Power Engineering Review, vol. 16, no. 5, pp. 5-, May 1996, doi: 10.1109/MPER.1996.491910.

[6] Xuzhu Dong, Yilu Liu and J. G. Kappenman, "Comparative analysis of exciting current harmonics and reactive power consumption from GIC saturated transformers," 2001 IEEE Power Engineering Society Winter Meeting. Conference Proceedings (Cat. No.01CH37194), 2001, pp. 318-322 vol.1, doi: 10.1109/PESW.2001.917055.

[7] Meta-R-321, The Late-Time (E3) High-Altitude Electromagnetic Pulse (HEMP) and Its Impact on the U.S. Power Grid, January 2010

[8] J. G. Kappenman et al., "GIC mitigation: a neutral blocking/bypass device to prevent the flow of GIC in power systems," in IEEE Transactions on Power Delivery, vol. 6, no. 3, pp. 1271-1281, July 1991, doi: 10.1109/61.85876.

[9] A. H. Etemadi and A. Rezaei-Zare, "Optimal Placement of GIC Blocking Devices for Geomagnetic Disturbance Mitigation," in *IEEE Transactions on Power Systems*, vol. 29, no. 6, pp. 2753-2762, Nov. 2014, doi: 10.1109/TPWRS.2014.2309004.

[10] Hao Zhu and T. Overbye, "Blocking device placement for mitigating the effects of geomagnetically induced currents," *2016 IEEE Power and Energy Society General Meeting (PESGM)*, 2016, pp. 1-1, doi: 10.1109/PESGM.2016.7741143.

[11] A. H. Naghshbandy, A. G. Baayeh and A. Faraji, "Blocking DC Flux due to Geomagnetically Induced Currents in the Power Network Transformers," 2019 International Power System Conference (PSC), 2019, pp. 772-776, doi: 10.1109/PSC49016.2019.9081556.

[12] M. Nazir, K. Burkes and J. H. Enslin, "Converter-Based Solutions: Opening New Avenues of Power System Protection Against Solar and HEMP MHD-E3 GIC," in *IEEE Transactions on Power Delivery*, vol. 36, no. 4, pp. 2542-2549, Aug. 2021, doi: 10.1109/TPWRD.2020.3016207.

[13] B. Kovan and F. de León, "Mitigation of Geomagnetically Induced Currents by Neutral Switching," in IEEE Transactions on Power Delivery, vol. 30, no. 4, pp. 1999-2006, Aug. 2015, doi: 10.1109/TPWRD.2015.2434411.

[14] https://www.mathworks.com/help/sps/powersys/ref/saturabletransformer.html

[15] DOE: Physical Characteristics of HEMP Waveform Benchmarks for Use in Assessing Susceptibilities of the Power Grid, Electrical Infrastructures, and Other Critical Infrastructure to HEMP Insults.

[16] T. J. Overbye, et. al. "Power Grid Geomagnetic Disturbance (GMD) Modeling with Transformer Neutral Blocking and Live Grid Testing Results"

[17] Betts, John T., Practical Methods for Optimal Control and Estimation Using Nonlinear Programming, Second Edition

[18] An Introduction to Trajectory Optimization: How to Do Your Own Direct Collocation. Matthew Kelly SIAM Review 2017 59:4, 849-904 https://github.com/MatthewPeterKelly/OptimTraj

[19] A. Wächter and L. T. Biegler, On the Implementation of a Primal-Dual Interior Point Filter Line Search Algorithm for Large-Scale Nonlinear Programming, Mathematical Programming 106(1), pp. 25-57, 2006

[20] mexIPOPT, Enrico Bertolazzi Department of Industrial Engineering University of Trento

[21] https://www.mathworks.com/help/sps/powersys/ref/pisectionline.html

VII. Appendix

The standalone transformer case-study considered in Section III is reconsidered in this appendix with the inclusion of the 60Hz ac component ($v_a = 1$ p.u.) in addition to the E3a impulse. The resulting magnetizing flux for the transformer is shown in Fig. 11, which shows the case for: no mitigation, blocking capacitor, and optimal controller based on λ_m limits. It is clear from Fig. 11 that both the blocking capacitor and λ_m limit controller do a suitable job of preventing transformer saturation (the brief saturation in the blocking capacitor case at the start of the interval is due to the initialization of the ODE solver, not the E3a impulse).

The control effort required to obtain this response is shown in Fig. 12. These results are similar to the results shown in Section III, the primary difference between the two can be seen in the zoomed in subplot in Fig. 12. This shows the control effort near the peak of the E3a response, and instead of being a smooth function, the controller is seen to increase sharply during the parts of 60Hz cycle where the ac component and E3a component work together to push the transformer outside saturation limits, and then falls rapidly (due to minimum control effort objective) as the 60Hz component enters the part of the cycle that works against the E3a component.

Overall, it was found for the inclusion of the 60Hz component for the standalone transformer case-study did not have an outsized impact on the behavior of the optimal control results. Nevertheless, the generation of harmonics due to transformer saturation plays a key role in the degradation of grid resilience during a HEMP/event [6]. Thus, it is possible that 60Hz effects may play a more important role in different grid situations, and its inclusion here within the top-down optimal control framework serves as a useful demonstration.

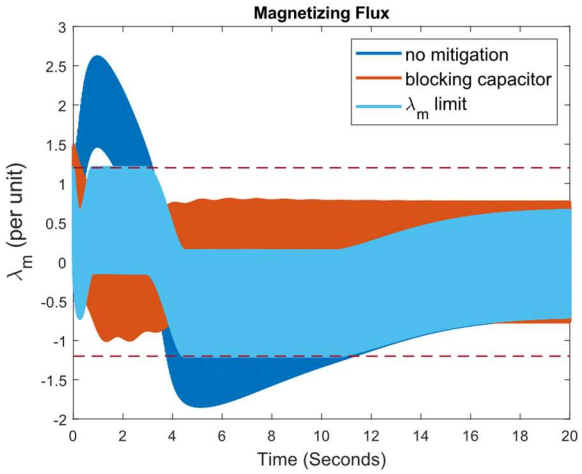

Fig. 11 – Transformer flux (60Hz+E3a)

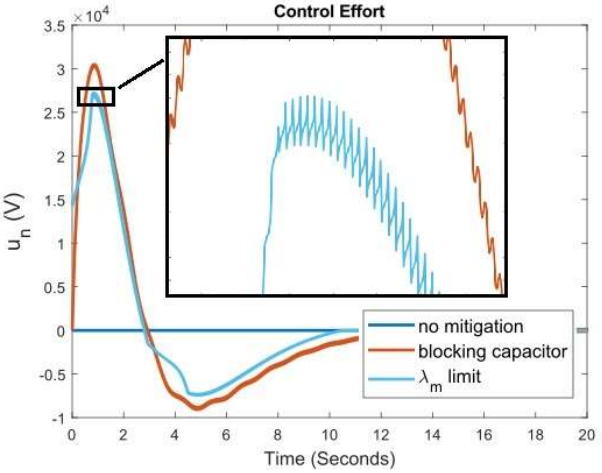

Fig. 12 – Control voltage (with zoomed subplot showing 60Hz response)